

**This item is the archived peer-reviewed author-version of:**

Corrosion protection of Cu by atomic layer deposition

**Reference:**

Cremers Véronique, Rampelberg Geert, Baert Kitty, Abrahams Shoshan, Claes Nathalie, Milagres de Oliveira Thais, Terryn Herman, Bals Sara, Dendooven Jolien, Detavernier Christophe.- Corrosion protection of Cu by atomic layer deposition  
Journal of vacuum science and technology: A: vacuum surfaces and films - ISSN 0734-2101 - 37:6(2019), 060902  
Full text (Publisher's DOI): <https://doi.org/10.1116/1.5116136>



## Corrosion protection of Cu by Atomic Layer Deposition

Véronique Cremers,<sup>1, 2</sup> Geert Rampelberg,<sup>1</sup> Kitty Baert,<sup>3</sup> Shoshan Abrahami,<sup>3</sup> Nathalie Claes,<sup>4</sup> Thais Milagres de Oliveira,<sup>4</sup> Herman Terryn,<sup>3</sup> Sara Bals,<sup>4</sup> Jolien Dendooven,<sup>1</sup> and Christophe Detavernier<sup>1</sup>

<sup>1</sup>*Department of Solid State Sciences, Ghent University, Krijgslaan 281/S1, B-9000 Ghent, Belgium*

<sup>2</sup>*SIM vzw, Technologiepark 48, 9052 Zwijnaarde, Belgium*

<sup>3</sup>*Research Group Electrochemical and Surface Engineering, Vrije Universiteit Brussel (VUB), Pleinlaan 2, 1050 Brussels, Belgium*

<sup>4</sup>*Electron Microscopy for Materials Research (EMAT), University of Antwerp, Groenenborgerlaan 171, 2020 Antwerp, Belgium*

(Dated: 15 August 2019)

Atomic Layer Deposition (ALD) is a vapor phase technique which is able to deposit uniform, conformal thin films with an excellent thickness control at the atomic scale. 18 nm thick Al<sub>2</sub>O<sub>3</sub> and TiO<sub>2</sub> coatings were deposited conformally and pinhole free onto micron-sized Cu powder, using trimethylaluminum (TMA) and tetrakis(dimethylamido)titanium(IV)(TDMAT) respectively as a precursor and de-ionized water as a reactant. The capability of the ALD coating to protect the Cu powder against corrosion was investigated. Therefore the stability of the coatings was studied in solutions with different pH in the range of 0-14, and in-situ raman spectroscopy was used to detect the emergence of corrosion products of Cu as an indication that the protective coating starts to fail.

Both ALD coatings provide good protection at standard pH values in the range of 5-7. In general, the TiO<sub>2</sub> coating shows a better barrier protection against corrosion than the Al<sub>2</sub>O<sub>3</sub> coating. However for the most extreme pH conditions, pH 0 and pH 14, the TiO<sub>2</sub> coating starts also to degrade.

## Corrosion protection of Cu by Atomic Layer Deposition

### I. INTRODUCTION

Atomic Layer Deposition (ALD) is a chemical vapor growth method for the deposition of uniform thin films with thickness control at the atomic scale.<sup>1,2,3,4,5</sup> Due to the self-limiting nature of the gas-solid surface reactions in ALD, it is possible to grow highly conformal inorganic coatings onto large scale substrates with complex topologies.<sup>6,7,8,9</sup> In recent years, ALD has extensively been explored to study the surface functionalization of powders.<sup>10</sup> ALD coating of powders is used in a wide range of applications as e.g. for the protection of metal powder against oxidation<sup>11,12</sup>, for the encapsulation of moisture sensitive powder<sup>13</sup> and catalytic activation.<sup>14</sup> In this research, we investigate the ability of ALD to protect Cu powder against corrosion.

Copper is a metal with a high thermal conductivity and is used for a wide range of applications in water plumbing and heat exchanger.<sup>15,16,17</sup> Copper is reasonably corrosion resistant, however it has a finite corrosion rate in pure water which causes defects over time. The corrosion rate depends on the temperature and the pH of the solution and the dissolved species in the water.<sup>18,19,20,21</sup> Barrier coatings are often used in order to protect the substrate against corrosion. A wide range of techniques have been used for the deposition of barrier coatings, e.g. chemical vapor deposition (CVD),<sup>22,23,24</sup> electrodeposition<sup>25,26,27</sup> and plasma treatment.<sup>28</sup> Recently, a lot of research has been done on ALD coatings protecting aluminum (alloys)<sup>29,30</sup>, silver articles<sup>31</sup> and stainless steel<sup>32</sup> against corrosion. Abdulgatov et al.<sup>33</sup> studied ZnO, Al<sub>2</sub>O<sub>3</sub>, TiO<sub>2</sub> and Al<sub>2</sub>O<sub>3</sub> layers with a capping of TiO<sub>2</sub> on a planar Cu substrate to prevent water corrosion. The combined ALD layer of Al<sub>2</sub>O<sub>3</sub> and TiO<sub>2</sub> was able to protect the copper for 80 days in water at a temperature of 90°C. Daubert et al.<sup>34</sup> studied the stability against corrosion of different ALD coatings: Al<sub>2</sub>O<sub>3</sub>, TiO<sub>2</sub>, ZnO, HfO<sub>2</sub>, and ZrO<sub>2</sub>. They found the best initial corrosion protection by the Al<sub>2</sub>O<sub>3</sub> and HfO<sub>2</sub> coatings. However HfO<sub>2</sub> coatings showed the best film quality after an extended exposure.

In this work, we aim to deposit uniform, conformal and pinhole free layers of Al<sub>2</sub>O<sub>3</sub> and TiO<sub>2</sub> on micron-sized Cu powder. We will investigate if the ALD coatings can protect the complex 3D-shaped powder surface against corrosion. The stability of the coatings was investigated in solutions with a pH value in the range of 0-14, using in-situ Raman spectroscopy.



## II. EXPERIMENTAL

The ALD depositions were carried out in a home-built rotary pump-type ALD reactor for powders.<sup>35,36</sup> The powder is contained in a stainless steel container with a membrane at the front and the back. In this way, the gasses can flow through the membranes and the container, where it will react with the powder, while the powder is forced to stay in the container. During the deposition, the powder container is rotating (rotation speed of 35 rotations per minute) to ensure a proper agitation of the powder which enables the deposition of a conformal coating on the powder. Contrary to the often used fluidized bed reactors,<sup>37</sup> the ALD reactor used in this study is a pump-type reactor, which means that no purge gas is used to evacuate the ALD chamber after a precursor/reactant pulse. Instead, a turbomolecular pump is used to pump the reaction products and excess of precursor/reactant molecules away. In that way, the base pressure of the reactor was kept at  $1 \times 10^{-5}$  mbar.

During this research, dendritic Cu powder was used with an average particle size  $< 45 \mu\text{m}$ . (Sigma Aldrich) The  $\text{Al}_2\text{O}_3$  coating was deposited using TMA (trimethylaluminium, TMA, 97% Sigma Aldrich) as a precursor and de-ionized  $\text{H}_2\text{O}$  as a reactant. The partial pressure was regulated with a needle valve and kept at  $1 \times 10^{-3}$  mbar for TMA and  $2 \times 10^{-3}$  mbar for  $\text{H}_2\text{O}$ . One ALD cycle consisted of 20s TMA pulse time - 60s pump time - 20s  $\text{H}_2\text{O}$  pulse time - 60s pump time. The  $\text{Al}_2\text{O}_3$  deposition consisted of 150 ALD cycles targeting a coating thickness of 18 nm. The titaniumoxide coating was deposited using TDMAT (tetrakis(dimethylamido)titanium(IV), 99,999%, Sigma Aldrich) as a precursor and de-ionized  $\text{H}_2\text{O}$  as a reactant. The bubbler of the TDMAT precursor was heated to  $40^\circ\text{C}$ , to increase the partial pressure to  $5 \times 10^{-4}$  mbar. One ALD cycle consisted of 20s TDMAT pulse time - 60s pump time - 20s  $\text{H}_2\text{O}$  pulse time - 60s pump time. The  $\text{TiO}_2$  deposition consisted of 300 ALD cycles, targeting a coating thickness of 18 nm.

During the deposition, the temperature of the powder was kept at  $100^\circ\text{C}$ , using an external furnace. The precursor lines and the reactor walls were heated to  $90^\circ\text{C}$  to avoid the creation of coldspots, where the precursor/reactant possibly could condensate.

The presence of the coating was investigated using a FEI Quanta 200 F Scanning Electron Microscope (SEM) and Energy Dispersive X-ray spectroscopy (EDX) with the electron beam energy operated at 15 keV. To investigate the uniformity, conformality and the thickness of the coating, the coated Cu powder was studied with Transmission Electron Microscopy (TEM), using a FEI

## Corrosion protection of Cu by Atomic Layer Deposition

Osiris microscope with an operating voltage at 200kV. The particles were first crushed in a solution with ethanol after which the solution is deposited on the Au-TEM grid, in order to prepare the sample for the measurements. With high angle annular dark field scanning transmission microscopy (HAADF-STEM), one can distinguish the core materials from the coating, because the intensity is proportional to  $Z^2$  with Z the atomic number.

We also investigated the capacity of the coatings to act as a barrier to protect the powder against corrosion. Therefore, the stability of the coatings was studied at room temperature in several solutions with different pH values or anions with in-situ Raman spectroscopy. The Horiba Scientific LabRAM HR Evolution with excitation through a green laser (532nm) (max. 1mW - objective 50x) Raman spectroscopy was used. The effect of extreme pH conditions was investigated, using solutions of 1M HNO<sub>3</sub> and NaOH, resulting in a pH value of 0 and 14 respectively. By lowering the concentration of the previous solutions, less extreme conditions could be studied. Solutions with 10<sup>-2</sup>M of NaOH and HNO<sub>3</sub>, resulted in pH conditions of 2 and 12 respectively. Solutions in an intermediate pH range are studied with solutions of 10<sup>-2</sup> M NaNO<sub>3</sub> and 10<sup>-2</sup> M NaNO<sub>3</sub> with 10<sup>-3</sup> M NaOH resulting in a pH of 5 and 7. The effect of a chloride environment on the ALD coating was studied in a 0.5M NaCl solution (standard corrosive).

The suspensions were prepared in small bottles (5mg/ml). At different exposure times, a small amount of the Cu-powder was put on a cavity microscope slide in a drop of solution and Raman measurements had been performed.

### III. RESULTS AND DISCUSSION

HAADF-STEM measurements were performed to determine whether the particles were coated in a uniform, conformal way. EDX elemental maps gave a fast indication about the presence of the coating. In Figure 1a the HAADF-STEM image and EDX mappings are shown for a Cu powder grain, coated with Al<sub>2</sub>O<sub>3</sub>. The mapped intensities for Al, O and Cu are shown. Al and O signals are clearly visible around the particle, confirming the presence of the Al<sub>2</sub>O<sub>3</sub> coating.

In Figure 1b an HAADF-STEM image and EDX mapping are shown for a Cu particle, coated with TiO<sub>2</sub>. The mapped intensities of Ti, O and Cu are shown. Ti and O can be observed, indicating the presence of the TiO<sub>2</sub> coating. Both EDX-mappings demonstrate the presence of an uniform coating.

By the combination of STEM imaging with different tilt angles and EDX analysis, one can observe

## Corrosion protection of Cu by Atomic Layer Deposition

[H]

FIG. 3. Raman spectra of uncoated Cu powder (a), Cu powder coated with 18 nm of  $\text{Al}_2\text{O}_3$  (b) and Cu powder coated with 18 nm of  $\text{TiO}_2$  (c) suspended in a solution with pH 12.

that for both cases the ALD coating is uniform and conformal on the entire particle outer surface.

FIG. 1. HAADF-STEM image and EDX-mapping of Cu powder coated with 150 ALD cycles of TMA/ $\text{H}_2\text{O}$  (a) and 300 ALD cycles of TDMAT/ $\text{H}_2\text{O}$  (b).

FIG. 2. HAADF-STEM image of Cu powder coated with 150 cycles of TMA/ $\text{H}_2\text{O}$  (a) and 300 cycles of TDMAT/ $\text{H}_2\text{O}$ .

The thickness of the coating layers was determined based on HAADF-STEM images, as shown in Figure 2 for the Cu powder coated with  $\text{Al}_2\text{O}_3$  (a) and the powder coated with  $\text{TiO}_2$  (b). A clear difference in intensity between the  $\text{Al}_2\text{O}_3$  respectively  $\text{TiO}_2$  layer and the Cu particle, makes it possible to determine the thickness of the coating. The thickness of the coating was measured for different particles on different positions. The average coating thickness of the  $\text{Al}_2\text{O}_3$  coating was  $19.8 \pm 0.7\text{nm}$  after a deposition of 150 ALD cycles, corresponding with a growth per cycle of 0.132 nm which is in agreement with the growth per cycle of 0.133 nm for the same ALD process under similar conditions, reported in literature.<sup>38</sup> The  $\text{TiO}_2$  coating has an average thickness of  $18.5 \pm 0.6\text{ nm}$  after a deposition of 300 ALD cycles, corresponding to a growth per cycle of 0.062 nm. This value is in agreement with the growth per cycle of 0.065 nm reported for the TDMAT/ $\text{H}_2\text{O}$  depositions with similar process parameters.<sup>39</sup>

*a. Raman spectroscopy* The stability of both ALD coatings was tested under different pH conditions, in the range of pH 0 to pH 14. Raman spectroscopy was performed after several time steps. Depending on the pH of the solution and the presence of different anions, different copper corrosion products can be formed.<sup>40</sup> As an example, Figure 3 shows the Raman spectra (normalized) of the uncoated Cu powder (a), the Cu powder coated with  $\text{Al}_2\text{O}_3$  (b) and the Cu powder coated with  $\text{TiO}_2$  in a pH environment of 12. After two days, the uncoated Cu powder starts to corrode as indicated by the mixed copper oxide  $\text{Cu}_4\text{O}_3$  detected by Raman spectroscopy. After 4 days, the Cu sample coated with  $\text{Al}_2\text{O}_3$  turned black and a mixture of  $\text{Cu}_4\text{O}_3$  and CuO

## Corrosion protection of Cu by Atomic Layer Deposition

[H]

FIG. 4. Corrosion-stability of uncoated Cu powder (a), Cu powder coated with 18 nm of  $\text{Al}_2\text{O}_3$  (b) and Cu powder coated with 18 nm of  $\text{TiO}_2$  (c) exposed to solutions with a pH in the range of 0-14. A green square indicates that no corrosion products could be detected in the Raman spectra. A red dot indicates the occurrence of a corrosion product in the Raman spectra.

TABLE I. Raman fingerprint of copper corrosion products.

Copper corrosion product	Characteristic Wavenumbers ( $\text{cm}^{-1}$ ) <sup>41,42</sup>
CuO	296 - 346 - 631
$\text{Cu}_2\text{O}$	218 - 410 - 630
$\text{Cu}_4\text{O}_3$	540
$\text{Cu}_2\text{OH}_3\text{Cl}$	515 - 3312 - 3354 - 3441

could be measured at the powder. Later, the CuO contribution became stronger. In contrast, the Cu powder coated with  $\text{TiO}_2$  remains stable for 15 days, no corrosion products could be detected and no color changes could be observed. Table I gives an overview of the observed corrosion products with corresponding characteristic wavelength.

Figure 4 shows an overview of the corrosion resistance of the uncoated and coated powders suspended in a solution with a pH in the range of 0-14. A green square indicates that the powder is still resistant to the corresponding pH after the indicated time, as indicated by the absence of detectable corrosion products in the Raman spectra. A red circle indicates the presence of features related to corrosion products in the corresponding Raman spectrum.

In the nitric acid,  $\text{HNO}_3$  (pH 0), the uncoated powder started to degrade after 1h. The Cu powder coated with  $\text{Al}_2\text{O}_3$  dissolved completely after 20h. Only a blue solution of  $\text{Cu}(\text{NO}_3)_2$  remains. After 20h, also the Cu powder coated with  $\text{TiO}_2$  becomes darker and starts slowly to degrade by forming  $\text{Cu}(\text{NO}_3)_2$ .

In the NaOH solution (pH 14), the Cu powder coated with  $\text{Al}_2\text{O}_3$  turned black after 20h and  $\text{Cu}_2\text{O}$  as corrosion product could be observed. In contrast, the Cu powder coated with  $\text{TiO}_2$  remained reddish and no corrosion products could be identified. In a pH 2 solution, the Cu powder coated with  $\text{Al}_2\text{O}_3$  started to degrade after 4 days and  $\text{Cu}_2\text{O}$  could be measured (after 2 days for uncoated

## Corrosion protection of Cu by Atomic Layer Deposition

[H]

FIG. 5. Raman spectra of the Cu powders in an acid solution (pH 2) (a) and chloride solution (0.5 M NaCl) (b) from the moment the corrosion products have been detected.

Cu). The Cu powder coated with TiO<sub>2</sub> remained stable after 15 days. Only after 4 weeks, a weak Cu<sub>2</sub>O-signal was measured. This is illustrated in Figure 5a.

In the pH 5 and 7 solutions, the blank Cu powder started to degrade after 4 days forming Cu<sub>2</sub>O. The Cu powder coated with Al<sub>2</sub>O<sub>3</sub> coating started to degrade after a week in the pH 5 solution, by forming Cu<sub>2</sub>O. After 4 weeks, this powder started also to degrade in the pH 7 solution, reacting to CuO. In contrast, the Cu powder coated with TiO<sub>2</sub> remained stable for 4 weeks in these neutral solutions.

The last corrosion test in NaCl, showed the formation of Cu<sub>2</sub>(OH)<sub>3</sub>Cl at the uncoated Cu powder after 3 days. After one week, this corrosion product plus Cu<sub>2</sub>O is also found at the Al<sub>2</sub>O<sub>3</sub> coated powder and just after 4 weeks a weak signal is noticed at the TiO<sub>2</sub> coated powder, as is illustrated in Figure 5b.

*b. Pourbaix diagram* The stability of a metal-aqueous interaction system is often summarized in a Pourbaix diagram.<sup>40</sup> It is a type of phase diagram, where the regions of immunity, passivation and corrosion are shown as a function of the pH (acidity) and  $E_h$  (standard hydrogen electronic potential). In the immunity region, no metal dissolution occurs, in contrast to the corrosion region where active metal dissolution occurs. In the passivation region, a protective metal-oxide film is formed which prevents metal dissolution. The Pourbaix diagrams predict that the Al<sub>2</sub>O<sub>3</sub> coating will only be stable for a pH range of 4-9,<sup>43</sup> while the TiO<sub>2</sub> coating will be stable for the entire pH range.<sup>44</sup> The studied ALD TiO<sub>2</sub> coating stayed stable in a pH of 2 and 12 in contrast to the Al<sub>2</sub>O<sub>3</sub> coating as predicted by the pourbaix diagrams. For the solutions with the most extreme pH of 0 and 14, we would expect the TiO<sub>2</sub> coating to remain stable, however degradation occurs. We have to remark that Pourbaix diagrams are derived for crystalline metal(oxide)s, but the deposited ALD coatings are amorphous and have a lower density compared to bulk TiO<sub>2</sub>, potentially explaining the reduced stability of the TiO<sub>2</sub> coating under the most extreme conditions.





Corrosion protection of Cu by Atomic Layer Deposition

#### IV. CONCLUSION

Micron-sized Cu powder was coated with circa 18 nm of Al<sub>2</sub>O<sub>3</sub> and TiO<sub>2</sub> using a pump-type rotary ALD reactor. SEM/EDX showed the presence of the coatings and HAADF-STEM and EDX measurements illustrated the uniformity and conformality of both coatings. To investigate whether the coatings can protect the Cu powder against corrosion, the stability of the coated powder was tested in solutions with different pH values and in standard NaCl solution. In-situ Raman spectroscopy was used to detect corrosion products when the coating starts to fail and the powder begins to corrode.

For non-extreme pH values, both ALD coatings provide a good protection against corrosion, which suggests the pinhole free nature of the coating. In general a better barrier performance is found for the TiO<sub>2</sub> coated Cu powder. However, in the most extreme pH conditions of pH 0 and pH 14, the TiO<sub>2</sub> coating starts to degrade too, in contrast to bulk TiO<sub>2</sub> which remains stable as shown by Pourbaix diagrams in literature. The amorphous structure and the lower density of the TiO<sub>2</sub> ALD coating may cause this different behavior.

#### V. ACKNOWLEDGEMENT

The authors acknowledge financial support from the Strategic Initiative Materials in Flanders (SIM, SBO-FUNC project) and the Special Research Fund BOF of Ghent University (GOA 01G01513). J.D. acknowledges the Research Foundation Flanders (FWO-Vlaanderen) for a post-doctoral fellowship.

#### REFERENCES

- <sup>1</sup>T. Suntola, "Atomic layer epitaxy," Mater. Sci. Rep. **4**, 261 (1989).
- <sup>2</sup>R. Puurunen, "Surface chemistry of atomic layer deposition: A case study for the trimethylaluminum/water process," J. Appl. Phys. **97** (2005).
- <sup>3</sup>R. Johnson, A. Hultqvist, and S. Bent, "A brief review of atomic layer deposition: From fundamentals to applications," Mater. Today **17**, 236 (2014).
- <sup>4</sup>S. George, "Atomic Layer Deposition: An Overview," Chem. Rev. **110**, 111 (2010).

## Corrosion protection of Cu by Atomic Layer Deposition

- <sup>5</sup>V. Miikkulainen, M. Leskelä, M. Ritala, and R. Puurunen, "Crystallinity of inorganic films grown by atomic layer deposition: Overview and general trends," *J. Appl. Phys.* **113**, 021301 (2013).
- <sup>6</sup>C. Detavernier, J. Dendooven, S. Pulinthanathu Sree, K. Ludwig, and J. Martens, "Tailoring nanoporous materials by atomic layer deposition," *Chem. Soc. Rev.* **40**, 5242 (2011).
- <sup>7</sup>J. Elam, D. Routkevitch, P. Mardilovich, and S. George, "Conformal Coating on Ultrahigh-Aspect-Ratio Nanopores of Anodic Alumina by Atomic Layer Deposition," *Chem. Mater.* **15**, 3507 (2003).
- <sup>8</sup>J. Dendooven, K. Devloo-Casier, M. Ide, K. Grandfield, M. Kurttepel, K. Ludwig, S. Bals, P. Van Der Voort, and C. Detavernier, "Atomic layer deposition-based tuning of the pore size in mesoporous thin films studied by in situ grazing incidence small angle X-ray scattering," *Nanoscale* **6**, 14991 (2014).
- <sup>9</sup>V. Cremers, R. Puurunen, and J. Dendooven, "Conformality in atomic layer deposition: Current status overview of analysis and modelling," *Appl. Phys. Rev.* **6**, 021302 (2019).
- <sup>10</sup>D. Longrie, D. Deduytsche, and C. Detavernier, "Reactor concepts for atomic layer deposition on agitated particles: A review," *J. Vac. Sci. Technol. A* **32**, 010802 (2014).
- <sup>11</sup>C.-L. Duan, Z. Deng, K. Cao, H.-F. Yin, B. Shan, and R. Chen, "Surface passivation of Fe<sub>3</sub>O<sub>4</sub> nanoparticles with Al<sub>2</sub>O<sub>3</sub> via atomic layer deposition in a rotating fluidized bed reactor," *J. Vac. Sci. Technol. A* **34**, 04C103 (2016).
- <sup>12</sup>V. Cremers, A. Rampelberg, Barhoum, P. Walters, N. Claes, T. Milagres de Oliveira, G. Van Assche, S. Bals, J. Dendooven, and C. Detavernier, "Oxidation barrier of Cu and Fe powder by Atomic Layer Deposition," *Surf. Coat. Tech.* **349**, 1032 (2018).
- <sup>13</sup>N. Avci, J. Musschoot, P. F. Smet, K. Korthout, A. Avci, C. Detavernier, and D. Poelman, "Microencapsulation of Moisture-Sensitive CaS:Eu[2+] Particles with Aluminum Oxide," *J. Electrochem. Soc.* **156**, J333 (2009).
- <sup>14</sup>K. Leus, C. Krishnaraj, L. Verhoeven, V. Cremers, C. Detavernier, P. Dubruel, and P. Van Der Voort, "Catalytic carpets: Pt@MIL-101@electrospun PCL, a surprisingly active and robust hydrogenation catalyst," *J. Catal.* **360**, 81 (2008).
- <sup>15</sup>I. Vargas, D. Fischer, M. Alsina, J. Pavissich, P. Pasten, and G. Pizarro, "Copper Corrosion and Biocorrosion Events in Premise Plumbing," *Materials* **10**, 1036 (2017).
- <sup>16</sup>J.-G. K. J.-Y. Lee, S.-H. and Kim, "Investigation of pitting corrosion of a copper tube in a heating system," *Eng. Fail. Anal.* **17**, 1424 (2010).



## Corrosion protection of Cu by Atomic Layer Deposition

- <sup>17</sup>B. Lu, W. Meng, and F. Mei, "Experimental Investigation of Cu-Based, Double-Layered, Microchannel Heat Exchangers," *J. Micromech. Microeng.* **23**, 035017 (2013).
- <sup>18</sup>B. Jeon, S. Sankaranarayanan, A. van Duin, and S. Ramanathan, "Atomistic Insights Into Aqueous Corrosion of Copper," *J. Chem. Phys.* **134**, 234706 (2011).
- <sup>19</sup>S. Pehkonen, A. Palit, and X. Zhang, "Effect of Specific Water Quality Parameters on Copper Corrosion," *Corrosion* **58**, 156 (2002).
- <sup>20</sup>Y. Feng, K. Siow, W.-K. Teo, K.-L. Tan, and A.-K. Hsieh, "Corrosion Mechanisms and Products of Copper in Aqueous Solutions at Various pH Values," *Corrosion* **53**, 389 (1997).
- <sup>21</sup>N. Boulay and M. Edwards, "Role of Temperature, Chlorine, and Organic Matter in Copper Corrosion By-Product Release in Soft Water," *Water. Res.* **35**, 683 (2001).
- <sup>22</sup>A. Sanjurjo, B. Wood, K. Lau, G. Tong, D. Choi, M. McKubre, H. Song, and N. Church, "Titanium-Based Coatings on Copper," *Surf. Coat. Tech.* **49**, 110 (1991).
- <sup>23</sup>G. Kalita, M. Ayhan, S. Sharma, S. Shinde, D. Ghimire, K. Wakita, M. Umeno, and M. Tanemura, "Low temperature deposited graphene by surface wave plasma CVD as effective oxidation resistive barrier," *Corros. Sci.* **78**, 183 (2014).
- <sup>24</sup>Y. Dong, Q. Liu, and Q. Zhou, "Corrosion behavior of Cu during graphene growth by CVD," *Corros. Sci.* **89**, 214 (2014).
- <sup>25</sup>Y. Liu, S. Li, J. Zhang, J. Liu, Z. Han, and L. Ren, "Corrosion inhibition of biomimetic superhydrophobic electrodeposition coatings on copper substrate," *Corros. Sci.* **94**, 190 (2015).
- <sup>26</sup>P. Herrasti, A. del Rio, and J. Recio, "Electrodeposition of homogeneous and adherent polypyrrole on copper for corrosion protection," *Electrochim. Acta* **52**, 6496 (2007).
- <sup>27</sup>G. He, S. Lu, W. Xu, S. Szunerits, R. Boukherroub, and H. Zhang, "Controllable growth of durable superhydrophobic coatings on a copper substrate via electrodeposition," *Phys. Chem. Chem. Phys.* **17**, 10878 (2015).
- <sup>28</sup>Y. Lin and H. Yasuda, "Effect of plasma polymer deposition methods on copper corrosion protection," *J. Appl. Polym. Sci.* **60**, 543 (1995).
- <sup>29</sup>M. Anderson, B. Aitchison, and D. Johnson, "Corrosion Resistance of Atomic Layer Deposition-Generated Amorphous Thin Films," *ACS Appl. Mater. Inter.* **8**, 30644 (2016).
- <sup>30</sup>S. Potts, L. Schmalz, M. Fenker, B. Díaz, J. Światowska, V. Maurice, A. Seyeux, P. Marcus, G. Radnóczy, L. Tóth, and W. Kessels, "Ultra-Thin Aluminium Oxide Films Deposited by Plasma-Enhanced Atomic Layer Deposition for Corrosion Protection," *J. Electrochem. Soc.* **158**, C132 (2011).



## Corrosion protection of Cu by Atomic Layer Deposition

- <sup>31</sup>S. Park, G. Han, H. Choi, F. Prinz, and J. Shim, "Evaluation of atomic layer deposited alumina as a protective layer for domestic silver articles: Anti-corrosion test in artificial sweat," *Appl. Surf. Sci.* **441**, 718 (2018).
- <sup>32</sup>C. Shan, X. Hou, and K.-L. Choy, "Corrosion resistance of TiO<sub>2</sub> films grown on stainless steel by atomic layer deposition," *Surf. Coat. Tech.* **202**, 2399 (2008).
- <sup>33</sup>A. Abdulagatov, Y. Yan, J. Cooper, Y. Zhang, Z. Gibbs, A. Cavanagh, R. Yang, Y. Lee, and S. George, "Al<sub>2</sub>O<sub>3</sub> and TiO<sub>2</sub> Atomic Layer Deposition on Copper for Water Corrosion Resistance," *ACS Appl. Mater. Inter.* **3**, 4593 (2011).
- <sup>34</sup>J. Daubert, G. Hill, H. Gotsch, A. Gremaud, J. Ovental, P. Williams, C. Oldham, and G. Parsons, "Corrosion Protection of Copper Using Al<sub>2</sub>O<sub>3</sub>, TiO<sub>2</sub>, ZnO, HfO<sub>2</sub>, and ZrO<sub>2</sub> Atomic Layer Deposition," *ACS Appl. Mater. Inter.* **9**, 4192 (2017).
- <sup>35</sup>D. Longrie, D. Deduytsche, J. Haemers, K. Driesen, and C. Detavernier, "A rotary reactor for thermal and plasma-enhanced atomic layer deposition on powders and small objects," *Surf. Coat. Tech.* **213**, 183 (2012).
- <sup>36</sup>G. Rampelberg, D. Longrie, D. Deduytsche, and C. Detavernier, "Plasma enhanced atomic layer deposition on powders," *ECS Transactions* **64**, 51 (2014).
- <sup>37</sup>H. Tiznado, D. Domínguez, F. Muñoz-Muñoz, J. Romo-Herrera, R. Machorro, O. E. Contreras, and G. Soto, "Pulsed-bed atomic layer deposition setup for powder coating," *Powder Technol.* **267**, 201 (2014).
- <sup>38</sup>M. Groner, F. Fabreguette, J. Elam, and S. George, "Low-Temperature Al<sub>2</sub>O<sub>3</sub> Atomic Layer Deposition," *Chem. Mater.* **16**, 639 (2004).
- <sup>39</sup>Q. Xie, J. Musschoot, D. Deduytsche, R. Van Meirhaeghe, C. Detavernier, S. Van den Berghe, Y.-L. Jiang, G.-P. Ru, B.-Z. Li, and W.-P. Qu, "Growth Kinetics and Crystallization Behavior of TiO<sub>2</sub> Films Prepared by Plasma Enhanced Atomic Layer Deposition," *J. Electrochem. Soc.* **155**, H688 (2008).
- <sup>40</sup>M. Pourbaix, *Atlas of Electrochemical Equilibria in Aqueous Solutions* (1st ed.; Pergamon Press: Oxford, U.K., 1966).
- <sup>41</sup>L. Debbichi, M. Marco de Lucas, J. Pierson, and P. Krüger, "Vibrational Properties of CuO and Cu<sub>4</sub>O<sub>3</sub> from First-Principles Calculations, and Raman and Infrared Spectroscopy," *J. Phys. Chem. C* **116**, 10232 (2012).
- <sup>42</sup>V. Hayez, *Use of micro-Raman spectroscopy for the study of the atmospheric corrosion of copper alloys of cultural heritage*, Ph.D. thesis, Vrije Universiteit Brussel, Belgium (2006).

This is the author's peer reviewed, accepted manuscript. However, the online version of record will be different from this version once it has been copyedited and typeset.  
PLEASE CITE THIS ARTICLE AS DOI: 10.1116/1.5116136

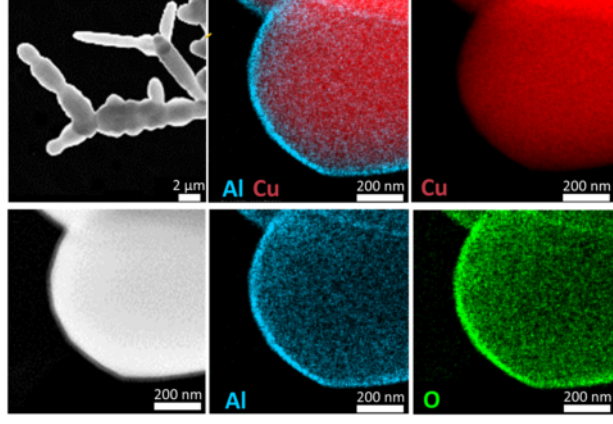
## Corrosion protection of Cu by Atomic Layer Deposition

<sup>43</sup>K. Mutombo and M. Du Toit, *Arc Welding* (IntechOpen, Rijeka, 2011) p. 183.

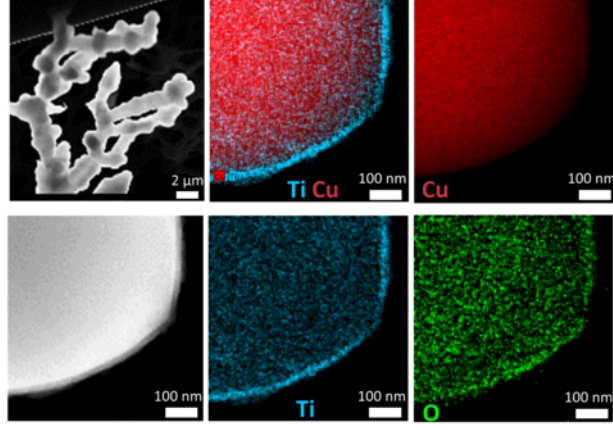
<sup>44</sup>A. Scheurmann and P. MCIntyre, “Atomic Layer Deposited Corrosion Protection: A Path to Stable and Efficient Photoelectrochemical Cells,” *J. Phys. Chem. Lett.* **7**, 2867 (2016).

<sup>45</sup>E. Schindelholz, E. Spoerke, H.-D. Nguyen, J. Grunlan, S. Qin, and D. Bufford, “Extraordinary Corrosion Protection from Polymer–Clay Nanobrick Wall Thin Films,” *ACS Appl. Mater. Inter.* **10**, 21799 (2018).

This is the author's peer reviewed, accepted manuscript. However, the online version of record will be different from this version once it has been copyedited and typeset.  
PLEASE CITE THIS ARTICLE AS DOI: 10.1116/1.5116136

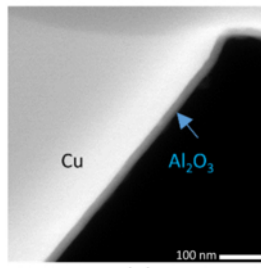


(a)

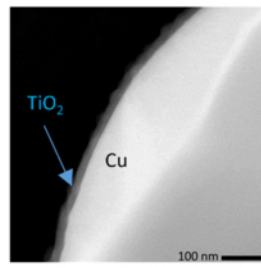


(b)

This is the author's peer reviewed, accepted manuscript. However, the online version of record will be different from this version once it has been copyedited and typeset.  
PLEASE CITE THIS ARTICLE AS DOI: 10.1116/1.5116136

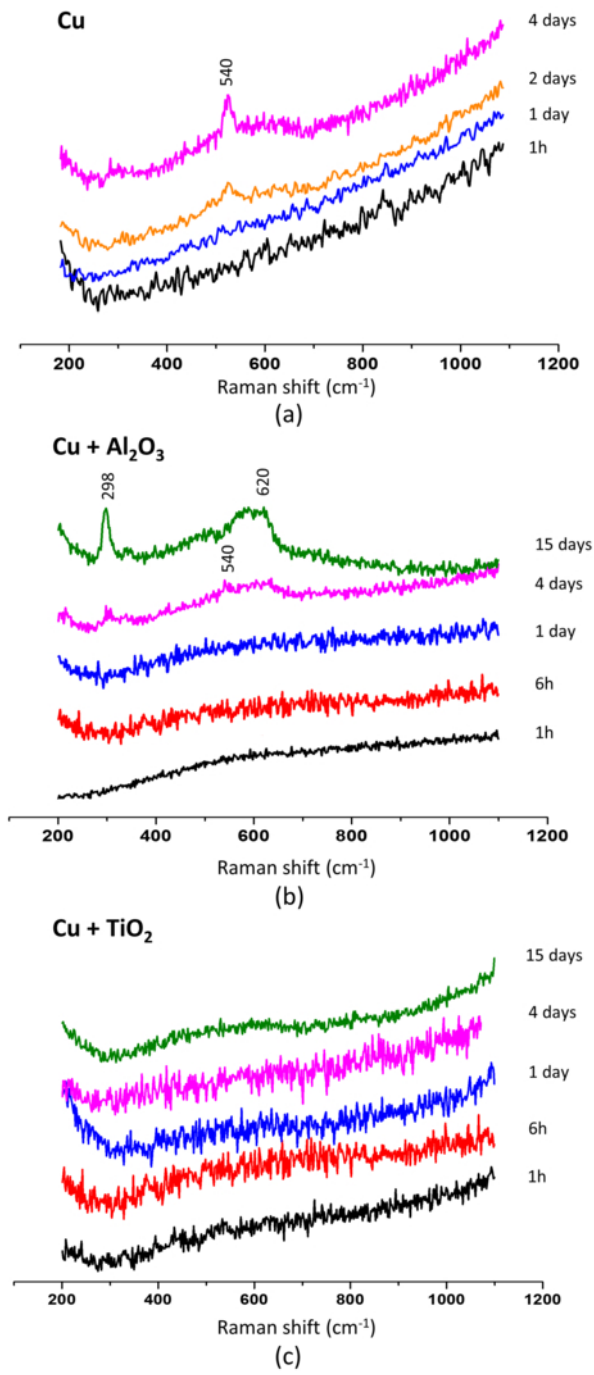


(a)



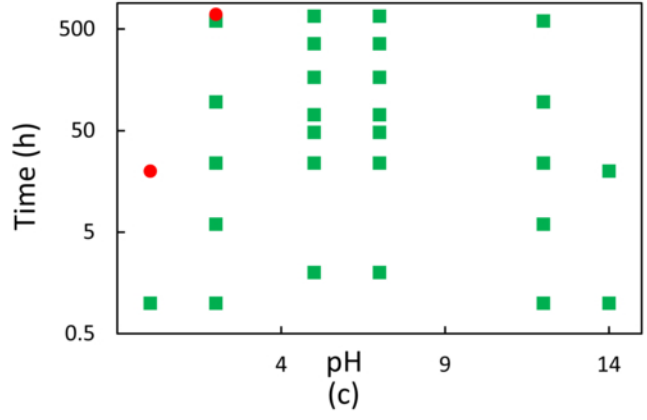
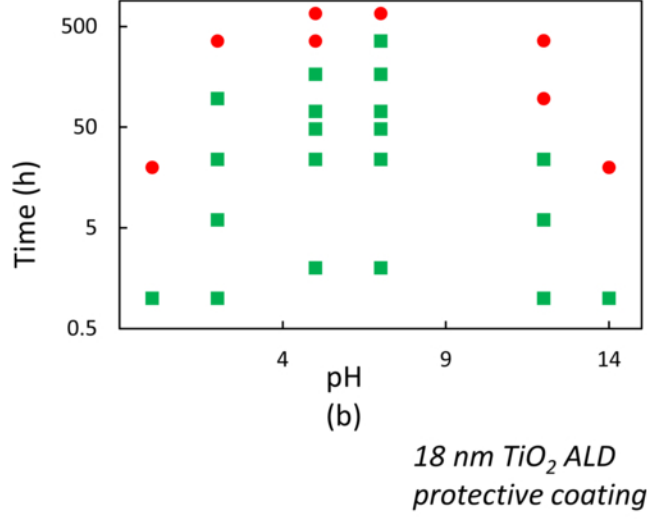
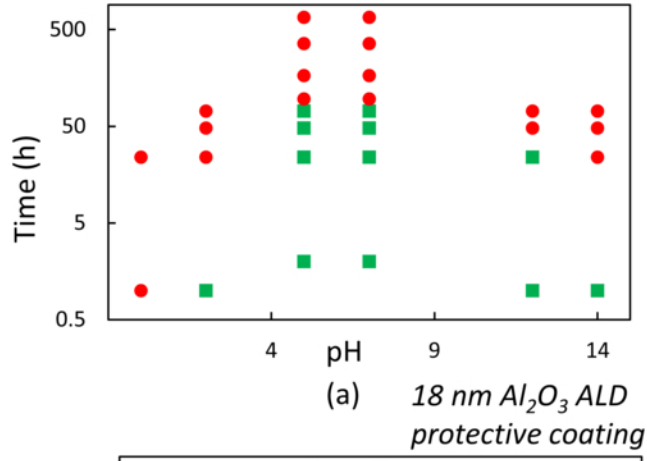
(b)

This is the author's peer reviewed, accepted manuscript. However, the online version of record will be different from this version once it has been copyedited and typeset.  
PLEASE CITE THIS ARTICLE AS DOI: 10.1116/1.5116136





This is the author's peer reviewed, accepted manuscript. However, the online version of record will be different from this version once it has been copyedited and typeset.  
PLEASE CITE THIS ARTICLE AS DOI: 10.1116/1.5116136



This is the author's peer reviewed, accepted manuscript. However, the online version of record will be different from this version once it has been copyedited and typeset.  
PLEASE CITE THIS ARTICLE AS DOI: 10.1116/1.5116136

